The Astrophysical Journal, 682:593–601, 2008 July 20

MOST[1] SPACE-BASED PHOTOMETRY OF THE TRANSITING EXOPLANET SYSTEM HD 189733: PRECISE TIMING MEASUREMENTS FOR TRANSITS ACROSS AN ACTIVE STAR

Eliza Miller-Ricci
Harvard-Smithsonian Center for Astrophysics, 60 Garden Street, Cambridge, MA 02138; emillerricci@cfa.harvard.edu

Jason F. Rowe
University of British Columbia, 6224 Agricultural Road, Vancouver, BC V6T 1Z1, Canada

Dimitar Sasselov
Harvard-Smithsonian Center for Astrophysics, 60 Garden Street, Cambridge, MA 02138

Jaymie M. Matthews
University of British Columbia, 6224 Agricultural Road, Vancouver, BC V6T 1Z1, Canada

Rainer Kuschnig
Department of Physics and Astronomy, University of British Columbia, 6224 Agricultural Road, Vancouver, BC V6T 1Z1, Canada

Bryce Croll
Department of Astronomy and Astrophysics, University of Toronto, 50 Saint George Street, Toronto, ON M5S 3H4, Canada

David B. Guenther
Department of Astronomy and Physics, St. Mary's University, Halifax, NS B3H 3C3, Canada

Anthony F. J. Moffat
Département de Physique, Université de Montréal, C.P. 6128, Succursale Centre-Ville, Montreal, QC H3C 3J7, Canada

Slavek M. Rucinski
David Dunlap Observatory, University of Toronto, P.O. Box 360, Richmond Hill, ON L4C 4Y6, Canada

Gordon A. H. Walker
Department of Physics and Astronomy, University of British Columbia, 6224 Agricultural Road, Vancouver, BC V6T 1Z1, Canada

and

Werner W. Weiss
Institut für Astronomie, Universität Wien, Türkenschanzstrasse 17, A-1180 Vienna, Austria
Received 2007 April 12; accepted 2008 February 13

ABSTRACT

We have measured transit times for HD 189733b passing in front of its bright ($V = 7.67$), chromospherically active, and spotted parent star. Nearly continuous broadband optical photometry of this system was obtained with the *Microvariability and Oscillations of Stars* (*MOST*) space telescope during 21 days in 2006 August, monitoring 10 consecutive transits. We have used these data to search for deviations from a constant orbital period which can indicate the presence of additional planets in the system that are as yet undetected by Doppler searches. There are no transit timing variations above the level of ±45 s, ruling out super-Earths (of masses 1–4 $M_\oplus$) in the 1:2 and 2:3 inner resonances, and planets of 20 $M_\oplus$ in the 2:1 outer resonance of the known planet. We also discuss complications in measuring transit times for a planet that transits an active star with large starspots, and how the transits can help constrain and test spot models. This has implications for the large number of such systems expected to be discovered by the *COROT* and *Kepler* missions.

Subject headings: methods: data analysis — planetary systems — stars: individual (HD 189733)

Online material: color figures

1. INTRODUCTION

While ground-based radial velocity (RV) and photometric transit surveys have unearthed more than 200 extrasolar planets in just over the last decade,[2] the ability to detect planets similar to the Earth, in size and mass, has so far remained out of reach of both of these methods. However, the potential to discover planets comparable to the mass of the Earth currently exists through measurements of transit timing variations (TTVs) in known transiting planetary systems (Agol et al. 2005; Holman & Murray 2005; Heyl & Gladman 2007). In addition, nearly continuous photometry from space currently offers the precision and time coverage to search for Earth-size transiting planets (e.g., Barge et al. 2005; Croll et al. 2007).

A summary of the TTV method is as follows. The motion of a transiting planet whose orbit is perturbed by another planet in the system will not have a constant period. These changes in period occur on the level of seconds to hours (Agol et al. 2005; Holman & Murray 2005) depending on the mass and orbital parameters

[1] Based on data from the *MOST* satellite, a Canadian Space Agency mission, jointly operated by Dynacon Inc., the University of Toronto Institute for Aerospace Studies, and the University of British Columbia, with the assistance of the University of Vienna.

[2] See the Extrasolar Planets Encyclopedia at http://www.exoplanet.eu.

of the perturbing planet. By measuring the times for repeated transits of a known planet, one can at least constrain, if not unambiguously determine, the mass and semimajor axis of the perturbing body. Such TTV analyses can be performed on any exoplanet for which high-quality photometry is available for a number of transits. For the TrES-1 system an analysis of transit timings has been carried out by Steffen & Agol (2005), with the result that any companion planet in an orbit nearby to the known close-in giant planet must have a mass comparable to or less than that of Earth. For the HD 209458 system, Agol & Steffen (2007) and Miller-Ricci et al. (2008) have placed limits on the existence of additional low-mass planets down to less than an Earth mass in certain resonant orbits, using data from the *Hubble Space Telescope* (*HST*) and the *Microvariability and Oscillations of Stars* (*MOST*; Walker et al. 2003; Matthews et al. 2004) satellite, respectively. Here we apply a similar TTV analysis to the HD 189733 system to search for low-mass companion planets in orbits neighboring the known transiting planet.

HD 189733 is currently the brightest star ($V = 7.67$) known to harbor a transiting exoplanet (Bouchy et al. 2005). This fact, along with its position on the sky and the short (2.2 day) period of its transiting planet, makes it ideally suited for observations by the *MOST* satellite. *MOST* observed HD 189733 for 21 days in 2006 August, monitoring 10 consecutive planetary transits. By determining the timings of these transits we are able to place limits on the presence of additional planets in this system down to a level of several Earth masses in certain orbits.

Another characteristic of HD 189733 that makes it unique among the known transiting systems is that the star has surface spots which modulate its optical light at a level of about 3% during the stellar rotation cycle (Winn et al. 2006; J. M. Matthews et al. 2008, in preparation). This level of variability is consistent with the fact that the star is known to be relatively active, with a chromospheric activity index $S = 0.525$ (Wright et al. 2004). The presence of starspots on HD 189733 must be taken into account when fitting the light curves of the exoplanetary transits, since the shapes of individual transits can be affected (1) if they coincide with the planet's passage in front of a spot, or (2) if the underlying variability of the star is rapid enough to affect the fit to the transit.

The *COROT* (Baglin 2003; Barge et al. 2005) and *Kepler* (Borucki et al. 2004; Basri et al. 2005) satellite missions (launched 2006 December 27 and scheduled for launch in 2009 February, respectively) are both expected to detect a large number of new transiting planets to add to an already growing list. One exciting prospect of these new systems is that each of them should be suited to the type of TTV analysis that we present in this paper, since high-quality observations of multiple consecutive transits will be available. Many of these newly discovered exoplanets may transit in front of chromospherically active stars like HD 189733, since such stars are commonplace, and neither the *COROT* nor *Kepler* team has done a priori selection of quiet stars for their transit searches. In the following TTV analysis, we incorporate the intrinsic variability of HD 189733, in an attempt to quantify the effects that this may have on the measurement of transit times. This provides valuable experience for future observations of transits of active spotted stars by *COROT*, *Kepler*, and ground-based surveys.

2. *MOST* PHOTOMETRY

HD 189733 was observed by *MOST* nearly continuously for 21 days from 2006 July 31 to August 21. The photometry was collected in *MOST*'s Direct Imaging mode operating with a single CCD, where a defocused stellar image was recorded on a subraster of the *MOST* Science CCD. The exposure time for individual frames was 1.5 s (read time is negligible), and 14 consecutive images were "stacked" on board the satellite to achieve high signal-to-noise ratio with a time sampling interval of 21 s. The original plan for the duration of the HD 189733 run was 14 days, and the first 14 days of observation have a duty cycle of 94%. When examination of the light curve showed the obvious spot modulation, the run was extended for 7 more days, by sharing each *MOST* satellite orbit ($P = 101.4$ minutes) with the next scheduled Primary Science Target. Therefore, the last week of data have a reduced duty cycle of 46%, and the observations were restricted to *MOST* orbital phases of highest scattered earthshine (with a resulting increase in photometric scatter). Still, the time sampling and photometric precision for the final week of observations remain excellent and are sufficient for analysis of the transit light curve.

The data were reduced in the same way as described by Rowe et al. (2006) for the transiting system HD 209458. The stellar fluxes were extracted by aperture photometry (aperture radius = 4 pixels; stellar image FWHM $\sim$ 2.5 pixels), which gives better results than point-spread function (PSF) fitting. The raw instrumental light curve was decorrelated against the sky background as described by Rowe et al. (2006), and also against the location of the PSF centroid on the CCD.

The reduced light curve of HD 189733 is shown in the top panel of Figure 1. It is immediately apparent that the star itself was variable during the *MOST* observations at a level of approximately 30 mmag. The shape and timescale of these variations are consistent with rotational modulation due to spots on the surface of HD 189733.

3. FITTING THE TRANSIT LIGHT CURVE

To fit and time the observed transits properly, the underlying variability of the host star must be subtracted from the light curve. We have adopted two independent approaches: (1) We smooth the out-of-transit (OOT) light curve using as a kernel a weighted average of the data covering one *MOST* satellite orbital period (about 101 minutes) centered on each data point. For the in-transit data, we linearly interpolate the smoothed data through the time of transit. Finally, we subtract the resulting smoothed light curve from the data. (2) We apply a filtered discrete Fourier transform to the data, in which we remove all power except at the orbital period of the exoplanet HD 189733b and its harmonics. We use the orbital period determined by Winn et al. (2007).

The filtered light curves resulting from these two methods are shown in the middle and bottom panels of Figure 1, respectively. In the subsequent TTV analysis, we use both of the independently normalized light curves and find consistent results from each.

3.1. *Transit Model*

In computing the transit times, we compare the *MOST* data against a model transit light curve, constructed using the formalism set forth in Mandel & Agol (2002). To determine the system parameters describing this model—stellar mass and radius (M_* and R_*), planetary radius (R_p), orbital inclination (i), orbital period (P), and stellar limb-darkening coefficients (c_1–c_4)—we proceed as follows.

Since M_* cannot be determined from photometry alone, we adopt the value from Bouchy et al. (2005) of $M_* = 0.82 \pm 0.03\ M_\odot$, which in turn was determined by fitting the star's observed spectral parameters against stellar evolution models. For R_*, R_p, and i, we take advantage of the high-quality photometry provided by *MOST* to do an independent fit to these parameters.

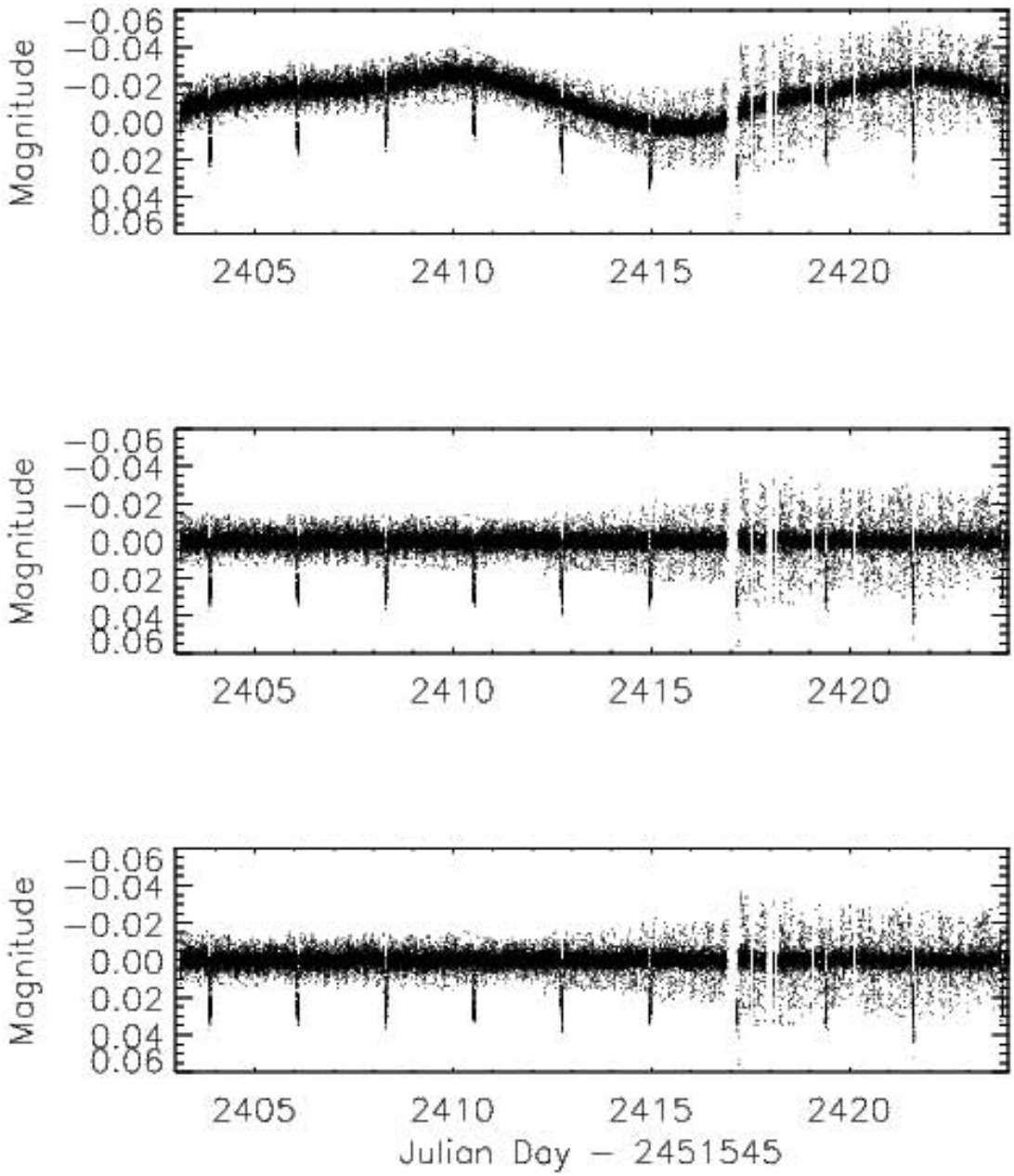

FIG. 1.—*Top*: *MOST* light curve of HD 189733. *Middle*: Light curve normalized by smoothing the OOT data and subtracting this smoothed curve. *Bottom*: Light curve normalized by applying a filtered Fourier transform to remove all power except at the orbital period of the planet and its harmonics.

To determine the transit parameters for the HD 189733 system, we use a maximum likelihood analysis to fit the data with the analytic model of Mandel & Agol (2002) and also add reflected light from the planetary companion (see J. M. Matthews et al. [2008, in preparation] for details). For priors on the stellar and planetary mass and radius as well as the orbital period and inclination of the planet, we adopt the values given in Winn et al. (2007). We obtain stellar and planetary radii of $0.749 \pm 0.009\ R_{\odot}$ and $1.192 \pm 0.019\ R_{\rm Jup}$ (equatorial radius), respectively, and we find the orbital inclination angle to be $85.70^{\circ} \pm 0.11^{\circ}$.

For the above analysis, we fixed the orbital period of HD 189733b at 2.2185733 ± 0.0000019 days (Winn et al. 2007). This value was determined by compiling all available transit times for fully observed transits over a period of more than a year, making it more precise than what could be obtained from a fit to the *MOST* light curve alone. In § 4 we present our own calculation of P by adding our transit times to the list of those previously available, and we find that the value we obtain is entirely consistent with the one we have chosen to use for our model transit light curve.

Since the *MOST* telescope has a custom broadband filter covering the range 350–700 nm, we cannot use standard tables of limb-darkening coefficients (such as those by Claret [2000]), which are only valid for standard filter systems. In addition, the quality of the *MOST* photometry is not high enough to observationally constrain limb-darkening parameters, especially given the wide bandpass of the instrument. We instead generate nonlinear limb-darkening parameters for HD 189733 from a synthetic spectrum, calculated from model atmospheres using the ATLAS 9 and ATLAS 12 codes by Kurucz (1995) and rewritten in FORTRAN 90 (J. Lester 2002, private communication). We employ a model with $T_{\rm eff} = 5000$ K, $\log g = 4.5$, microturbulence of 1 km s^{-1},

TABLE 1
Orbital and Physical Parameters for HD 189733

Parameter	Value
M_* ($M_\odot$)	0.82 ± 0.03[a]
R_* ($R_\odot$)	0.749 ± 0.009
R_{pl} (R_{Jup})	1.192 ± 0.019
i (deg)	85.70 ± 0.11
P (days)	2.2185733 ± 0.0000019[b]
c_1	0.825232
c_2	−0.977556
c_3	1.686737
c_4	−0.657020

Note.—The parameters c_1–c_4 are the nonlinear limb-darkening coefficients calculated for the *MOST* bandpass.
[a] From Bouchy et al. (2005).
[b] From Winn et al. (2007).

and solar metallicity, consistent with the stellar parameters for HD 189733 given by Bouchy et al. (2005) and Melo et al. (2006). The emergent spectrum is calculated at each of 17 values of $\mu = \cos\theta$ from the center of the star out to the limb, where θ is the angle relative to the normal. We then determine nonlinear limb-darkening coefficients (c_n) as a function of wavelength according to the law:

$$I(r) = \sum_{n=1}^{4} c_n \left(1 - \mu^{n/2}\right). \quad (1)$$

Finally, we multiply by the total throughput function for *MOST*, which includes the effects of the filter, optics, CCD, and its electronics. The resulting limb-darkening coefficients for the *MOST* bandpass, along with the other system parameters for the model light curve, are listed in Table 1. In Figure 2 the transit model is plotted over the binned (normalized) data, which have been folded at the orbital period of HD 189733b.

3.2. *Transit Times*

Using the transit model described above, we find the best-fit center-of-transit times for nine of the 10 transits observed by *MOST*. Transit 7 is omitted due to the fact that *MOST* was switching observing modes at this time to the dual-star mode. For the nine transits that have good time coverage, we compute the model light curve for times that correspond with each of the *MOST* data points. We next determine the center time for each transit at which the χ^2 value for the fit to the data is minimized.

The 1 σ error bars are calculated using a bootstrapping Monte Carlo simulation similar to the one described in Agol & Steffen (2007) according to the following sequence. For each transit we shift the residuals from the best-fitted transit model (and their associated errors) by a random number of points. We then add the new residuals onto the transit model and recalculate the center-of-transit time using the same procedure described above, thus maintaining the original point-to-point correlations. We perform this procedure 200 times for each transit, and the scatter in the obtained transit times sets our uncertainties. This allows us to account for the effects of correlated (red) noise in the *MOST* data set, which is due to the repeating pattern of stray light (satellite orbital modulation of scattered earthshine) as well as to other systematics that remain in the light curve including any residual intrinsic stellar variations.

TABLE 2
Best-Fit Transit Times

Transit Number	T_C (HJD)	σ (HJD)	Reduced χ^2
1	2,453,948.86962	±0.00043	0.82
2	2,453,951.08753	±0.00022	0.83
3	2,453,953.30630	±0.00030	0.88
4	2,453,955.52467	±0.00025	0.61
5	2,453,957.74331	±0.00027	0.76
6	2,453,959.96201	±0.00025	0.65
8	2,453,964.39811	±0.00044	1.12
9	2,453,966.61827	±0.00054	1.00
10	2,453,968.83608	±0.00037	0.97

Note.—Transit 7 has been omitted due to a large gap in the data at this time.

The resulting transit times are listed in Table 2. We show these measurements in an $O - C$ (observed time−computed time) diagram in Figure 3, where the expected time of each transit (for constant orbital period) has been subtracted from its observed time to search for transit timing deviations. The expected times of transit are calculated from the period and ephemeris that we present in § 4. In Figure 4 we once again present an $O - C$ diagram of the transit times for HD 189733b, but now including, as

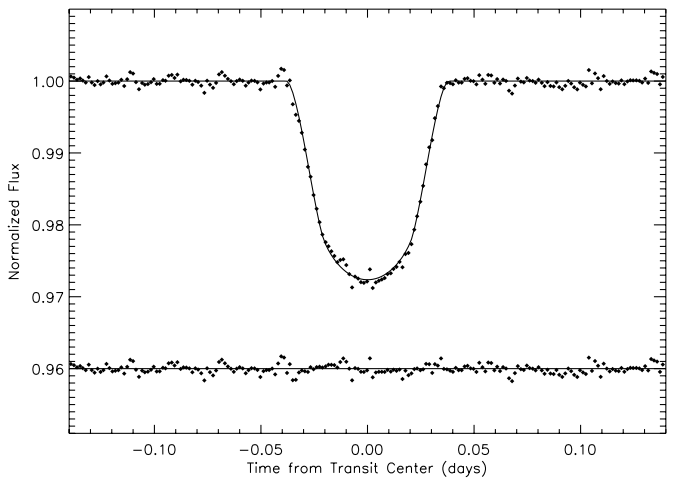

Fig. 2.—*Above*: The phase diagram of the *MOST* photometry of HD 189733, and the transit model, folded at the orbital period of the planet. The data have been averaged in 2 minute bins. *Below*: Residuals from the model.

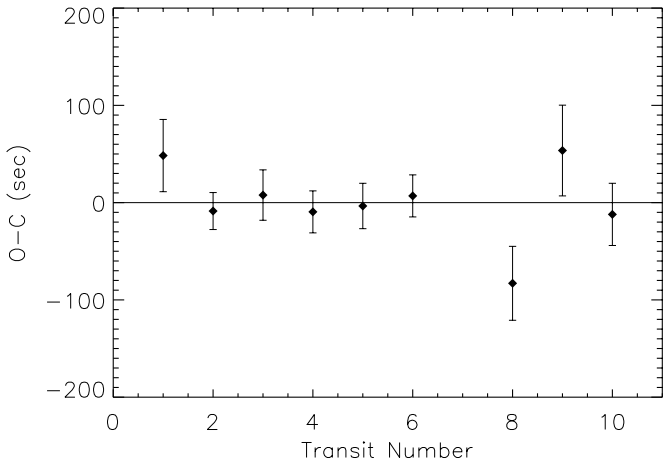

Fig. 3.—Deviation from predicted time of transit vs. transit number for transits of HD 189733b observed by *MOST* in 2006. The first six transits were fully sampled, while transits 8, 9, and 10 were only partially observed.

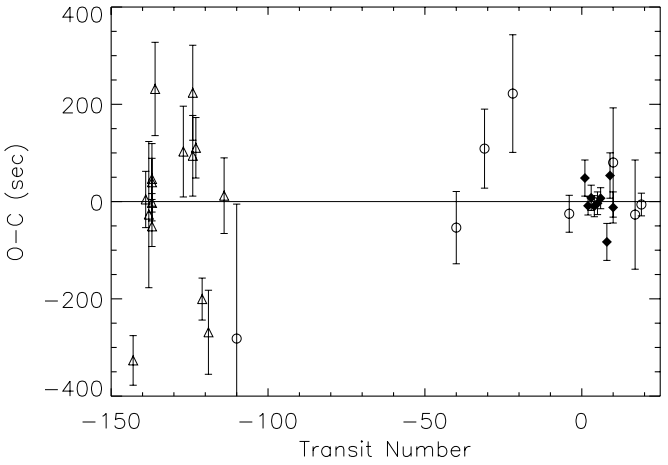

FIG. 4.—Deviation from predicted time of transit vs. transit number for all published well-sampled transits of HD 189733b. Data points from *MOST* are shown with diamonds, those from Winn et al. (2007) with circles, and those from Bakos et al. (2006) with triangles. Note that different methods have been used to compute the error bars for each individual data set. See the original papers for details. [*See the electronic edition of the Journal for a color version of this figure.*]

a reference, all available timing data from the literature in addition to our own.

For the first six transits observed by *MOST*, the transit times we obtain are consistent with a constant orbital period at the 1 σ level. The final three transits show increased scatter and uncertainty due to the fact that the light curve does not fully sample those transits, and portions of either ingress or egress are not observed. Gaps in the light curve during times when the planet is passing over the limb of the star can have a large effect on the accuracy to which transit times can be determined. This is due to the fact that fits to partial transits are highly sensitive to the values used for the limb-darkening parameters and the orbital inclination. If any of these deviate from their true values by even a small amount, the effect on the transit time can be substantial (see Miller-Ricci et al. 2008). We do not use the last three transits for our subsequent TTV analysis, as we expect the formal error bars in these cases to be underestimates.

4. TRANSIT TIMING VARIATIONS IN THE HD 189733 SYSTEM

The transit timing data on HD 189733 from *MOST* show no variations on three scales: (1) no long-term change in $P_{\rm orb}$ in about 15 yr at the 60 ms level; (2) no trend in transit timings during the first two weeks of the *MOST* run; and (3) no individual transit timing deviations at the 45 s level, with a string of five consecutive transits showing no timing deviations larger than 10 s. For illustration, see Figures 3 and 4.

4.1. *Long-Term Variations in the Orbital Period of HD 189733b*

We first address point (1) from the list above. Long-term variations in the orbital period could be caused by several effects, e.g., orbital decay of the planet HD 189733b (Sasselov 2003), or precession of its orbit (Miralda-Escudé 2002; Heyl & Gladman 2007). By combining archival *Hipparcos* photometry from 1991 and 1993 with the discovery data of Bouchy et al. (2005), Hébrard & Lecavelier Des Etangs (2006) have measured the orbital period of HD 189733b over a 15 yr baseline to be $2.218574^{+0.000006}_{-0.000010}$ days. Winn et al. (2007) independently determined the orbital period for HD 189733b to be 2.2185733 ± 0.0000019 days. Their measurement was based on a compilation of all available transit times for fully observed transits from their own work as well as from Bakos et al. (2006).

To further refine the value for the orbital period of HD 189733b and also to reduce the size of its associated error bar, we present here a new calculation of the period. We follow the same method as Winn et al. (2007) and use all available timing data for full transits of HD 189733b, adding our own data points from the first six transits observed by *MOST* to the list. We fit the resulting 18 transit times with a linear function of the form

$$T_c(N) = T_c(0) + PN, \tag{2}$$

where $T_c(0)$ is the epoch and N is the transit number. We choose $N = 0$ as the fourth transit observed by *MOST*, since this is the transit time known to the highest precision. The orbital period and epoch obtained from the fit are 2.2185733 ± 0.0000014 days and JD $2{,}453{,}955.52478 \pm 0.00010$, respectively. Our new value for the period is entirely consistent with all previous determinations. We have, however, reduced the size of the 1 σ error bar to 120 ms, now making this the most accurate value available for the orbital period of HD 189733b.

The star HD 189733 is estimated to have a mass of 0.82 $M_\odot$ with about 3% uncertainty (Bouchy et al. 2005; Bakos et al. 2006). With our stellar model for this mass and a planet mass of 1.15 $M_{\rm Jup}$, we can compute orbital decay rates. For the fastest possible orbital decay (high-dissipation linear model; Zahn 1977, 1989), we get a rate of 0.6 ms yr^{-1}. Currently available transit timing data for HD 189733b are not yet sensitive to long-term changes in P at this level. However, with the accumulation of future transit timing observations of this system, further constraints can be placed on this estimate.

4.2. *Short-Term Variations in the Orbital Period of HD 189733b Due to Additional Close-in Planets in the System*

The existing radial velocity curve for HD 189733 (Winn et al. 2006) excludes additional periodic variations (other than the known giant planet) larger than 10 m s^{-1} in amplitude and up to a period of about 40 days. This puts a limit on the mass of a possible long-period perturbing planet at about $M_{\rm pert} \gtrsim 10^{-4}\ M_\odot \simeq 0.1\ M_{\rm Jup} \simeq 32\ M_\oplus$. The TTV method is complimentary to the RV method in that it is generally more sensitive to smaller close-in perturbing planets. This is especially true in the case of the additional planet lying in a resonant orbit with the transiting planet, where the interactions between the two bodies are strongest. We use only the first six *MOST* transits here (see § 3.2), so the run can constrain only short-period perturbers in nearby resonances to HD 189733b, and periods shorter than about 6 days.

To determine what types of planets are ruled out by the *MOST* data, both in mass and orbits, we solve the classical N-body problem,

$$\frac{d^2x_i}{dt^2} = -\Sigma_{j=1;\,j\neq i}\, N\ \frac{Gm_j(x_i - x_j)}{|x_i - x_j|^3}, \tag{3}$$

where for three bodies, x describes the initial positions of the particles. A third body was inserted with an initially circular orbit, with periods ranging from 1 to 9 days in increments of 0.01 days, with masses from 1 to 100 $M_\oplus$ in 1 $M_\oplus$ increments, and on a coplanar orbit to HD 189733b. The solution was advanced at 1.0 s intervals for 100 orbits of HD 189733b ($\sim 2 \times 10^7$ s) using the LSODA routine from ODEPACK (Radhakrishnan & Hindmarsh

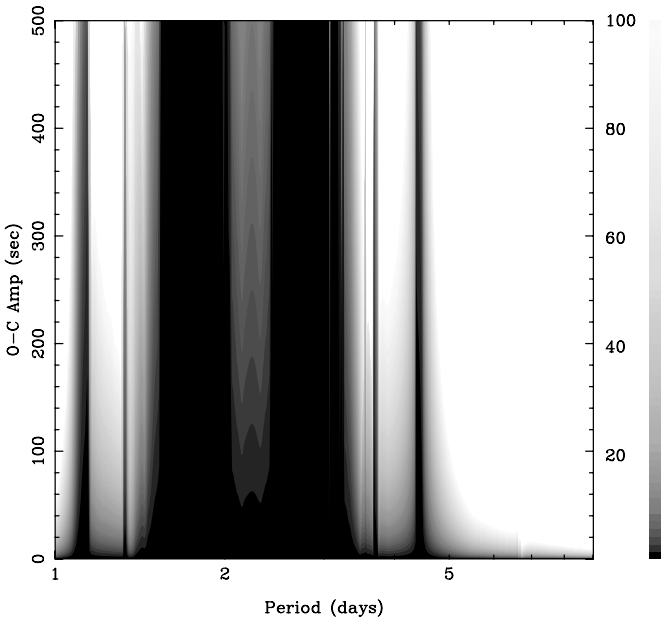

FIG. 5.—*N*-body results for maximum transit timing deviation vs. orbital period of the perturbing planet. The gray scale as defined on the right side of the plot indicates the mass of the perturbing planet (in $M_\oplus$). The *MOST* data, covering six orbits of HD 189733b, show no TTVs above the level of 45 s. [*See the electronic edition of the Journal for a color version of this figure.*]

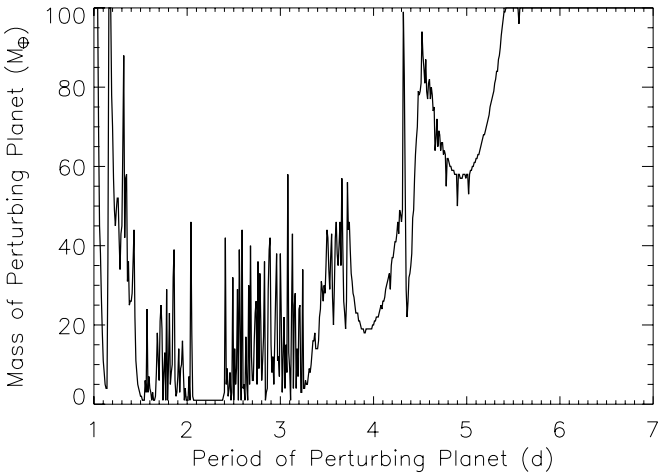

FIG. 6.—Maximum mass allowed for a perturbing planet in the HD 189733 system, which still remains consistent with the *MOST* transit times. Planets occupying the region of parameter space above the curve are ruled out by the available transit timing data with 95% confidence.

1993). $O - C$ values were then calculated by a linear interpolation to estimate the integration time when HD 189733b returns to the midpoint of crossing the disk of the star.

To determine the limits that transit timing data can place on additional planets in the HD 189733 system, we compute a Fourier transform of the $O - C$ series generated by the *N*-body code for each value of period and mass of the third body. We then extract the largest amplitude, as shown in Figure 5. However, we note that the largest amplitude of TTV can only be recovered from transit timing data if the entire libration period of the two-planet system is fully sampled. Otherwise, there is a risk that the times of largest transit timing deviations could be missed or passed over by the observations. Figure 5 therefore shows what types of limits on companion planets could be achieved if data were available for the full libration period of each hypothetical two-planet system. Given that the *MOST* transit timing data only cover six orbits of HD 189733b, we use the following procedure to determine what additional planets are ruled out from the system for cases where the libration period is longer than the 2 week duration of the *MOST* observing run.

We compare the *N*-body results against the *MOST* transit timing data to determine the maximum mass that an additional planet in the system can possess, while still remaining consistent with the data. This is achieved by removing any linear trends from each of the $O - C$ series generated by the *N*-body code, and then optimizing the agreement with the observed transit timing residuals by minimizing the χ^2 statistic. We then allow for the computed transit times to shift by an integer number of transits and determine the minimum value for χ^2 once the overall best fit is achieved. For each configuration, the perturbing planet is ruled out if the minimum in χ^2 is higher than a set threshold, implying that the results from the *N*-body simulation are inconsistent with the *MOST* transit times. Figure 6 shows the results of this process. The maximum mass of perturbing planet that remains consistent with the transit timing data at a confidence level of better than 5% is plotted as a function of the orbital period of the perturbing body. This corresponds to a χ^2 of less than 11.07 for the best fit of the *N*-body simulation to the data, on 5 degrees of freedom.

According to Figure 6, the TTV limits exclude perturbers of greater than 20 $M_\oplus$ for the exterior 2:1 mean motion resonance and greater than 8 $M_\oplus$ in the 3:2 resonance. In the interior 1:2 and 2:3 resonances, additional planets with masses larger than 4 and 1 $M_\oplus$ are ruled out, respectively. A range of intermediate orbits near the transiting planet HD 189733b are unstable for the lowest mass perturbers, resulting in ejections or collisions. Between 2.0 and 2.4 day periods we can rule out sub-Earth mass planets due to both TTV constraints and stability requirements. In addition, we can place more stringent limits than the 32 $M_\oplus$ value from radial velocity measurements in a number of nonresonant orbits with periods of up to 5 days.

For a perturbing planet on an eccentric orbit, the TTVs induced in the orbit of HD 189733b can be significantly larger than for the case of a circular orbit. Also, there is a reduced range of stable configurations for planets on eccentric orbits, especially for orbits interior to that of HD 189733b. We have performed a limited number of additional *N*-body simulations for perturbing planets in both mutually inclined orbits relative to the transiting planet, and in initially eccentric orbits. In almost all of these cases, we can place even stronger limits on the presence of additional planets in the HD 189733 system. In this sense, the limits that we have placed on perturbing planets from Figure 6 are robust limits across the entire range of eccentricity parameter space, since we initially only considered planets with zero eccentricity. Additional planets residing in eccentric or inclined orbits would have even larger effects on the transit times of HD 189733 than what we reported above.

5. CONSIDERATIONS DUE TO STARSPOTS

The amplitude of the intrinsic stellar variations during the *MOST* observing run suggests that HD 189733 may have had fairly large starspots of high flux contrast during this time. It is therefore quite possible that the exoplanet may have transited one or more spots during the 21 day run. This type of event would alter the shape of the transit light curve in a predictable way, and we can look for telltale signs of such an occurrence. From deviations in the shape of the transit light curve, Pont et al. (2007) observed HD 189733b occulting starspots in photometry from the *HST*. The approximate change in signal was 0.7%, and thus they inferred the presence of

TABLE 3
Transit Depth Measurements

Transit Number	Depth (%)
1	2.661 ± 0.048
2	2.605 ± 0.015
3	2.631 ± 0.019
4	2.670 ± 0.028
5	2.701 ± 0.023
6	2.694 ± 0.021

spots at least 80,000 km across (1.1 $R_{\rm Jup}$), given an inferred temperature of the spots that was 1000 K cooler than the star itself.

Were the transiting planet to have crossed over a starspot during the *MOST* observing run, the depth of the transit at this time would be shallower than otherwise predicted due to the fact that the planet would be passing in front of a cooler, hence optically dimmer, region of the photosphere. Since the lessening in transit depth would occur only during the portion of the transit when the planet is actually in front of the starspot and not necessarily during the entire transit, the overall effect when fitting the Mandel & Agol (2002) transit model to the light curve would be twofold. First, the shape of the transit would deviate from the form predicted by the transit model, resulting in a poorer goodness-of-fit (χ^2) value. Second, a shallower than normal overall depth would be needed to best describe a transit affected by a starspot.

Taking into account the second effect, we have examined the *MOST* data for variations in depth between successive transits to determine if such a spot-crossing event took place during the *MOST* observing run. For each of the six fully observed transits, we now allow for the depth of the transit, $(R_p/R_*)^2$, to be a free parameter in our fit. While the standard Mandel & Agol (2002) template transit model cannot predict the correct transit shape in the case where the planet crosses a starspot, this analysis still allows for an estimate as to whether there are significant changes in the average transit depth throughout the *MOST* observing run. To determine the size of the error bars of these measurements, we employ the same bootstrap method described above for the transit timing measurements. This once again allows us to account for correlated noise in the data, which can also affect the transit depth. The resulting values for transit depth are given in Table 3. The mean transit depth is 2.660%, with a mean uncertainty of ±0.027%. All six measurements are consistent with a constant depth at the 2 σ level.

With the current precision in our transit depth measurements, we note that we cannot detect changes in depth smaller than about 3% at the 3 σ level. Essentially, this means that the noise in the data could conceal the passage of HD 189733 over starspots smaller than approximately 0.2 $R_{\rm Jup}$ in radius, under the assumption that the starspots are 1000 K cooler than the rest of the photosphere (see discussion below). It is entirely possible that this type of small spot is present on the surface of HD 189733.

Croll et al. (2007) have obtained the best fit of the unfiltered *MOST* light curve to a simple spot model with two large starspots, obtaining a rotation period of $11.73^{+0.07}_{-0.05}$ days and a stellar rotational inclination of $59^{+3}_{-8}{}^\circ$. The spot model period is very close to the rotation period of $11.953^{+}_{-}0.09$ days determined by Henry & Winn (2008) from ground-based photometry spanning from 2005 October to 2007 July. However, the two values still differ by several sigma: a fact that may point to differential rotation for the set of starspots that was being observed. The Croll et al. (2007) model for HD 189733 assumes circular spots, solid-body surface rotation, and the possibility of evolution in spot size during the observations. The starspots are assumed to be 1000 K cooler than the rest of the photosphere, which is consistent with sunspots and with *HST* observations of the HD 189733 system (Pont et al. 2007). However, the starspot temperature cannot be determined uniquely from the *MOST* light curve, and there is a degeneracy between the sizes and temperatures of the spots.

As a demonstration of the power of studying transits in systems with spotted stars, we combine the *MOST* transit observations with the starspot analysis of Croll et al. (2007) to predict whether HD 189733b should have transited in front of one of the modeled starspots during the observing run. The spot model predicts the position and size of the two large starspots on the disk of HD 189733 at any time during the *MOST* run.

Using snapshots generated from the spot model discussed above, we can overlay the position of the transiting planet on an image of the stellar disk to see if HD 189733b is expected to have passed over either of the two large starspots, as shown in Figure 7. In this figure, it is possible to project the position of the planet on the star by the combination of three independent pieces of information. First, the sky projection angle between the orbital axis of the transiting planet and the stellar rotation axis of the star is known to be $\lambda = -1.4^\circ \pm 1.1^\circ$ (Winn et al. 2006). This value was determined by measuring the Rossiter-McLaughlin effect, which is the radial velocity distortion seen as a transiting planet occults the projected rotation profile of the star (see Ohta et al. 2005; Giménez 2006; Gaudi & Winn 2007). In addition, the stellar inclination angle (I_*) has been obtained from combining the measurement of $v \sin I_*$ (also from the Rossiter-McLaughlin effect; Winn et al. 2006) with the rotation period of star obtained by Croll et al. (2007). Finally, the inclination angle of the planet's orbit is known from fits to the transit light curve. The only remaining ambiguity lies in the fact that it is not known whether the transit crosses along a chord below or above the stellar equator. In Figure 7 we depict both cases.

From Figure 7 it can be seen that if HD 189733b were positioned above the stellar equator as it transits, it would have crossed one of the large starspots in the Croll et al. (2007) model during four out of the six fully observed transits. A complete occultation of a starspot comparably sized to the transiting planet would reduce the transit depth to 35% of its original value. Such a large effect would be readily noticeable by eye, and it has also been ruled out by the transit depth analysis presented above for the first six transits from the *MOST* light curve. We can therefore conclude that, if the Croll et al. (2007) model is correct, HD 189733b must transit below the stellar equator (as depicted in Fig. 7). In this case, the planet is not expected to cross over either of the large starspots, with the possible exception of transit 3. In this single case, the combined uncertainties in the spot model and the orbital inclination axis of the planet may allow for HD 189733b to transit across the southern hemisphere spot. There is no evidence in the light curve of transit 3 to suggest a full occultation of this starspot. However, a partial occultation cannot be ruled out at the precision of the *MOST* data, making this transit the most likely one to be affected by the presence of starspots, as determined by Croll et al. (2007).

As an additional consideration, in the event that the transiting planet crosses in front of a spot during ingress or egress, the change in depth of the transit from its expected value would be minimal. However, since such an event would change the shape of ingress or egress, the effect on the measured transit time would be considerable, as this is where the timing signal is most sensitive. This is not expected to have occurred in the HD 189733 system during the *MOST* observing run if the Croll et al. (2007) spot model is correct (see Fig. 7). However, a transit across a starspot

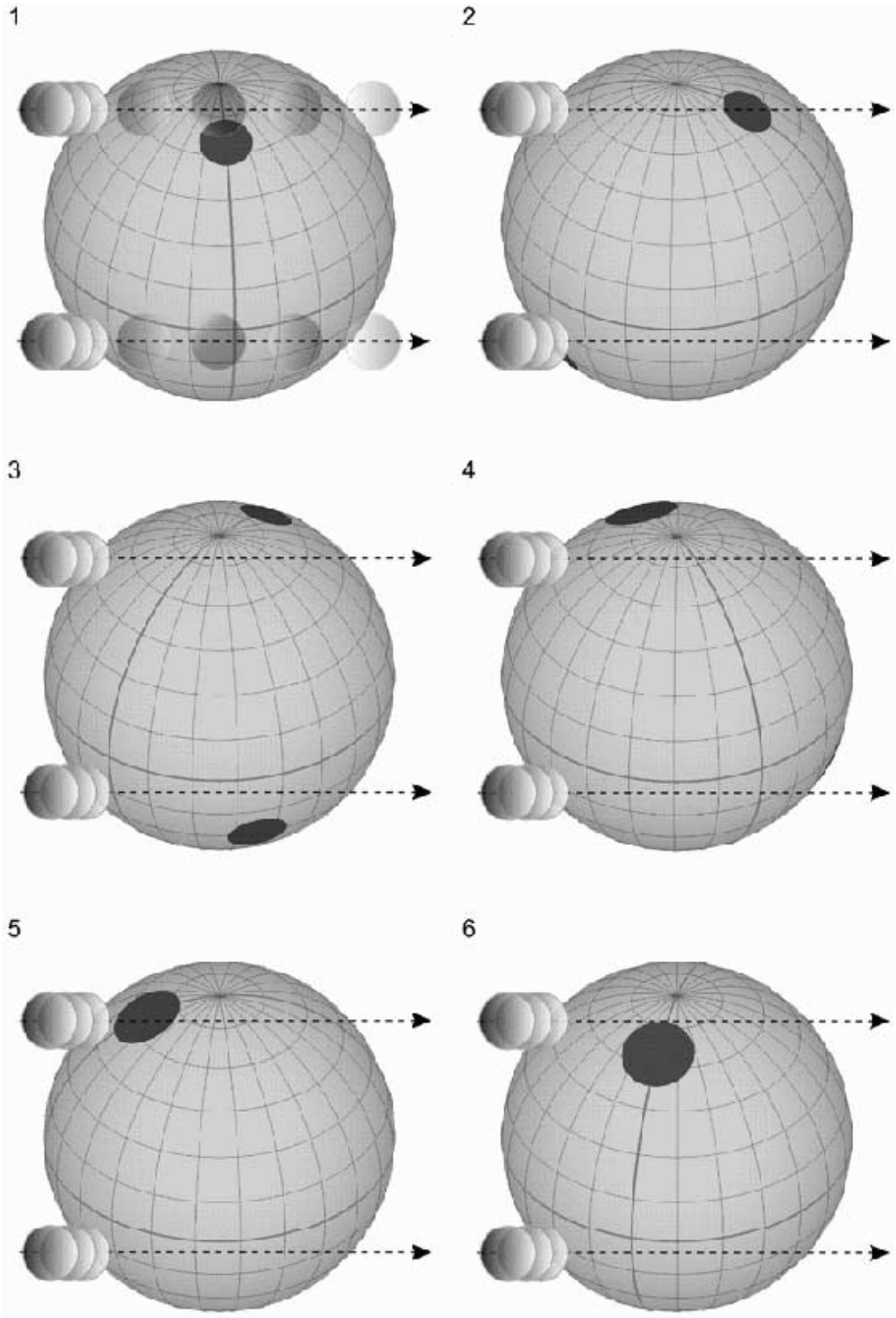

FIG. 7.—Snapshots from the HD 189733 starspot model by Croll et al. (2007) predicting the position of two large starspots at the times of the six complete transits observed by *MOST*. The projected tracks of the transiting planet are also shown, with two tracks for each transit, since only the orbital inclination, not the direction (north vs. south), is known. A northern hemisphere transit is ruled out if the Croll et al. model is correct, since effects of the passage over the large starspot in this region would be readily visible in the transit light curve. [*See the electronic edition of the Journal for a color version of this figure.*]

during ingress or egress could certainly take place during future observations. To determine the expected change to the transit time if such an event were to occur, we placed a simulated spot-crossing event into the data for one of the *MOST* transits. We found that a transit across a dark starspot with a diameter of 0.5 $R_{\rm Jup}$ during ingress could alter the measured transit time by more than a minute. Such an event remains virtually undetected by eye in the *MOST* data, but could be detected with space-based photometry of sufficient time sampling and precision such as that of *COROT*, *Kepler*, or the *HST*.

6. DISCUSSION AND CONCLUSIONS

We have measured accurate transit times for nine transits of HD 189733b observed by *MOST* during 21 days in 2006 August. For the six consecutive fully sampled transits we find no transit timing deviations above the 45 s level, allowing us to rule out certain configurations of additional perturbing planets in the system. We find no evidence for perturbing planets in the 1:2, 2:3, and 3:2 resonances down to the super-Earth level (4, 1, and 8 $M_{\oplus}$, respectively). In the exterior 2:1 resonance we rule out perturbing planets above the 20 $M_{\oplus}$ level, and we place the most stringent limits available on a range of nonresonant orbits with periods ranging from 1 to 5 days. In addition, we find no evidence for long-term changes in the orbital period of HD 189733b between 1991 and 2006, indicating no significant observable orbital decay or precession.

While HD 189733b is currently the only exoplanet known to transit a chromospherically active star, many more such systems may be discovered in the coming years, especially with the launches of the *COROT* and *Kepler* space missions. The occultation of a starspot changes the shape and depth of an observed transit, and passage of an exoplanet over a starspot during transit ingress or egress, changes the measured center time of the transit. This is of particular concern for lower precision photometry, where such deviations in the shape of the transit light curve may not be readily detectable, but the effects on the transit timing measurement can be significant.

For the transit timing analysis of the *MOST* light curve for HD 189733, we have been able to account for the presence of starspots in several ways. (1) The nearly continuous 21 day coverage and high precision of the data make it possible to subtract the intrinsic stellar variability before performing the transit timing analysis. (2) We have tested and constrained a two-spot model for the longer term variations in the *MOST* light curve (Croll et al. 2007), and combined it with spin-orbit alignment information from Rossiter-McLaughlin effect measurements (Winn et al. 2006). This has allowed us to project when and where the transiting planet would be expected to pass over a modeled starspot. (3) Our error analysis for the transit times takes into account correlated noise in the *MOST* light curve, due either to possible residual instrumental effects, or to passages of HD 189733b over small spots on the star that are below the detection threshold for this data set.

Transiting planetary systems such as HD 189733 point to the intriguing possibility that the transits themselves could be useful probes of the nature of spots and activity on the host star. High-quality photometry of future transits of this system could be used to "map" the surface brightness and geometry of spots in the part of the stellar disk traversed by the transiting planet.

We urge any observers reporting transit times for planets transiting active stars to carefully consider possible starspot effects in any observed deviant transit times before assuming the presence of a perturbing body in the system. The type of analysis presented in this paper can be implemented in principle for any system to rule out starspots as a cause of TTVs. This method necessitates a light curve taken with high photometric precision and complete time coverage over at least two stellar rotation periods, to detect and model the low-level variability of the star due to the motion of starspots across its surface. Such observations are best obtained from space or with a network of medium-aperture ground-based telescopes such as the planned Las Cumbres Observatory Global Telescope (Brown et al. 2006). Such data will help to make headway in the search for low-mass planets in known transiting systems, even in the case where the stars are chromospherically active.

We would like to thank Paul A. Kempton for his help in the graphical design of Figure 7. J. M. M., D. B. G., A. F. J. M., and S. M. R. acknowledge funding from the Natural Sciences and Engineering Research Council (NSERC) Canada. A. F. J. M. is also supported by FQRNT (Quebec). R. K. is supported by the Canadian Space Agency. W. W. W. is supported by the Austrian Research Promotion Agency (FFG) and the Austrian Science Fund (FWF P17580).

REFERENCES

Agol, E., & Steffen, J. H. 2007, MNRAS, 374, 941
Agol, E., Steffen, J., Sari, R., & Clarkson, W. 2005, MNRAS, 359, 567
Baglin, A. 2003, Adv. Space Res., 31, 345
Bakos, G. Á., et al. 2006, ApJ, 650, 1160
Barge, P., et al. 2005, in SF2A-2005: Semaine de l'Astrophysique Francaise, ed. F. Casoli et al. (Les Ulis: EDP Sciences), 193
Basri, G., Borucki, W. J., & Koch, D. 2005, NewA Rev., 49, 478
Borucki, W., et al. 2004, in Stellar Structure and Habitable Planet Finding, ed. F. Favata, S. Aigrain, & A. Wilson (ESA SP-538; Noordwijk: ESA), 177
Bouchy, F., et al. 2005, A&A, 444, L15
Brown, T. M., Taylor, S. F., Rosing, W., Mann, R., Trimble, V., & Farrell, J. A. 2006, BAAS, 56.05, 136
Claret, A. 2000, A&A, 363, 1081
Croll, B., et al. 2007, ApJ, 671, 2129
Gaudi, B. S., & Winn, J. N. 2007, ApJ, 655, 550
Giménez, A. 2006, ApJ, 650, 408
Hébrard, G., & Lecavelier Des Etangs, A. 2006, A&A, 445, 341
Henry, G. W., & Winn, J. N. 2008, AJ, 135, 68
Heyl, J. S., & Gladman, B. J. 2007, MNRAS, 377, 1511
Holman, M. J., & Murray, N. W. 2005, Science, 307, 1288
Kurucz, R. L. 1995, in ASP Conf. Ser. 78, Astrophysical Applications of Powerful New Databases, ed. S. J. Adelman & W. L. Wiese (San Francisco: ASP), 205
Mandel, K., & Agol, E. 2002, ApJ, 580, L171
Matthews, J. M., Kusching, R., Guenther, D. B., Walker, G. A. H., Moffat, A. F. J., Rucinski, S. M., Sasselov, D., & Weiss, W. W. 2004, Nature, 430, 51
Melo, C., Santos, N. C., Pont, F., Guillot, T., Israelian, G., Mayor, M., Queloz, D., & Udry, S. 2006, A&A, 460, 251
Miller-Ricci, E., et al. 2008, ApJ, 682, 586
Miralda-Escudé, J. 2002, ApJ, 564, 1019
Ohta, Y., Taruya, A., & Suto, Y. 2005, ApJ, 622, 1118
Pont, F., et al. 2007, A&A, 476, 1347
Radhakrishnan, K., & Hindmarsh, A. C. 1993, LLNL Rep. UCRL-ID-113855
Rowe, J. F., et al. 2006, ApJ, 646, 1241
Sasselov, D. D. 2003, ApJ, 596, 1327
Steffen, J. H., & Agol, E. 2005, MNRAS, 364, L96
Walker, G., et al. 2003, PASP, 115, 1023
Winn, J. N., et al. 2007, AJ, 133, 1828
———. 2006, ApJ, 653, L69
Wright, J. T., Marcy, G. W., Butler, R. P., & Vogt, S. S. 2004, ApJS, 152, 261
Zahn, J.-P. 1977, A&A, 57, 383
———. 1989, A&A, 220, 112